



The unit circle trap in boundary elements redux

G. Steven Gipson^{a,*}, B.W. Yeigh^b

^a*School of Civil and Environmental Engineering, Oklahoma State University, Stillwater, OK 74078-5033, USA*

^b*Office of the Vice President for Academic Affairs, Norwich University, USA*

Received 7 June 2005; accepted 30 August 2007

Abstract

This paper amplifies and subtends the BEM 27 paper: *The unit circle trap in boundary elements*. The paper deals with some traditional boundary element formulations that suffer from apparent instability problems when a unit circle is involved in the discretization. Such problems have been discussed informally and handled empirically by researchers, but apparently were never formalized with a numerical convergence study in the literature until done so by the authors in the proceedings of BEM 27. The present paper details how the problem arises, identifies sources for its occurrence, cites past allusions to the problem that have come to light since the presentation of the BEM 27 conference paper, and suggests remedies to avoid it. A theoretical outline is provided and extensive numerical case studies are presented. Particular emphasis is placed on the Poisson equation and its synthesis.

© 2007 Elsevier Ltd. All rights reserved.

Keywords: Unit circle; Poisson equation; Convergence; Boundary elements; Numerical instability

1. Introduction

This work focuses on an instability complaint that has been frequently discussed casually among boundary element researchers but apparently had been addressed sparsely in the formal literature and never in a formal numerical convergence study until the authors did so recently [1]. In fact, it was stated erroneously in that paper [1] that its contents were the only formal discussion of the issue in the literature. It was discovered later that the problem did have a modicum of coverage under titles different than that of “unit circle trap.” The issue has to do with solving the Poisson equation by boundary element analysis of the unit circle which is a typical case in normalized formulations involving circular geometry. The purpose of this paper is to give credit to other works dealing with the problem and to further elaborate one application in the Poisson equation where the problem arises and to illustrate why it happens. The cause is identified and a solution is proposed.

The example presented here is unusual in that it is best done using constant elements since, as will be

demonstrated, use of the more sophisticated, higher-order elements exacerbate the presence of an inherent stability problem. This lends credence to referring to the problem as a “trap.”

2. Background

A brief review of the derivation of the boundary element formulation for the Poisson equation is necessary to demonstrate the subtlety of the trap that ensues if one is not careful. The boundary element method is predicated upon defining a boundary value problem in terms of equations involving surface integrals. Ideally, one would like for the equations to be comprised solely of boundary integrals since this reduces the dimensionality of the problem. This reduction is not always possible and, in general, a set of equations arise that appear as

$$[H]\{u\} = [G]\{q\} + \{B\}. \quad (1)$$

We will use the 2D Poisson equation for illustration [2]. The general form of the differential equation is

$$\nabla^2 u(x, y) = b(x, y). \quad (2)$$

The $[H]$ and $[G]$ matrices in Eq. (1) result from boundary integrations. $\{u\}$ and $\{q\}$ are, respectively, boundary values

*Corresponding author. Tel.: +1 405 7445223.

E-mail address: gipson@okstate.edu (G. Steven Gipson).

of displacements (or temperatures, concentrations, etc.) and their normal gradients. $\{B\}$ is defined by domain integrals that are not dependent on any of the unknowns. The fundamental solution that makes this method work is usually taken to be that for a point source in free space

$$u_i^* = \frac{1}{2\pi} \ln |\vec{r} - \vec{r}_i|, \quad (3)$$

where $\vec{r} - \vec{r}_i$ is the position vector from point i to a general point in the plane.

Denoting the domain of the region by Ω and its boundary by Γ , we will assume the boundary is discretized into so-called constant elements for simplicity. In this case, the $[G]$ and $[H]$ matrix terms are denoted explicitly as integrals over boundary segments Γ_j

$$G_{ij} = \int_{\Gamma_j} u_i^* d\Gamma = \frac{1}{2\pi} \int_{\Gamma_j} \ln |\vec{r} - \vec{r}_i| d\Gamma \quad (4)$$

and

$$H_{ij} = \int_{\Gamma_j} \nabla u_i^* \cdot \vec{n} d\Gamma = \frac{1}{2\pi} \int_{\Gamma_j} \frac{(\vec{r} - \vec{r}_i) \cdot \vec{n}}{|\vec{r} - \vec{r}_i|^2} d\Gamma, \quad (5)$$

where \vec{n} is the outwardly directed unit normal vector on the boundary.

The domain integral terms are

$$B_i = \int_{\Omega} u_i^* b(x, y) d\Omega = \frac{1}{2\pi} \int_{\Omega} b(x, y) \ln |\vec{r} - \vec{r}_i| d\Omega. \quad (6)$$

Boundary element developers do not like domain integrals, so a great deal of energy has been expended converting terms like Eq. (6) into equivalent surface integrals. Fortunately, this can be done for many of the commonly occurring cases. For instance, if the known function $b(x, y)$ satisfies Laplace's equation,

$$\nabla^2 b = 0 \quad (7)$$

then Eq. (7) may be transformed using Green's theorem

$$B_i = \int_{\Omega} u_i^* b(x, y) d\Omega = \int_{\Gamma} (b \vec{\nabla} u_i^* \cdot \vec{n} - v_i^* \vec{\nabla} b \cdot \vec{n}) d\Gamma, \quad (8)$$

where v_i^* arises as a function that satisfies $\nabla^2 v_i^* = u_i^*$. From Eq. (3), it can be derived easily as

$$v_i^* = \frac{|\vec{r} - \vec{r}_i|^2}{8\pi} (\ln |\vec{r} - \vec{r}_i| - 1). \quad (9)$$

Forms of the function $b(x, y)$ that satisfy Eq. (7) include those with linear variations in x and y , and the all-important case $b(x, y) = \text{constant}$.

Most boundary element codes proceed by rewriting Eq. (1) so that unknown values of $\{u\}$ and $\{q\}$ are aligned on one side of the system with specified values of $\{q\}$ and $\{u\}$ on the other. The latter are augmented by the terms $\{B\}$ computed by Eq. (8) or by some other method. Denote the resulting vectors as $\{X\}$ and $\{F\}$, respectively. The net result is a system of equations

$$[A]\{X\} = \{F\} \quad (10)$$

which is then solved by some convenient means such as Gaussian elimination.

3. The problem

Engineers and scientists are notorious for verifying theories with textbook cases having simple exact solutions and/or using simple geometries. Classic examples include squares with unit sides or circles with unit radii. It is this last contingency that contributes to what appears initially to be a fallacy in the boundary element approach. To illustrate, consider the easily obtained exact polar coordinate solution of Eq. (2) on a circle of radius R with homogeneous Dirichlet boundary conditions and with $b = B_0$, a given constant,

$$u(r) = \frac{B_0}{4} (r^2 - R^2). \quad (11)$$

This problem arises routinely in electrostatics, steady-state heat transfer, groundwater flow, and torsion analysis of circular shafts. The normal derivative on the boundary is usually a pertinent quantity and Eq. (11) yields for this value:

$$q = \left. \frac{du}{dr} \right|_{r=R} = \frac{B_0 R}{2}. \quad (12)$$

This problem seems to be a perfect example for beta testing a boundary element program for proper assembly, solution, and consistency of results. Constructing a boundary element grid with equal-sized elements and *without* exploiting symmetry of any type serves this purpose. Every assembled equation should be the same and every calculated value of the boundary flux should be identical.

A typical element convergence study was performed. It involved progressing through several element types, progressing from the crude constant element to the linear, parabolic, cubic, and Overhauser cubic splines [3]. It was expected that the more sophisticated elements would be the better performers due to their ability to represent curved surfaces more accurately. Discretization examples are shown in Fig. 1.

None of the elements are capable of representing a circle exactly, so geometrical convergence was studied as well. For constant elements, three different criteria were used to construct the polygonal areas (Fig. 2(a)–(c)): (a) equating the radius of the circle to the radial distance of the midpoints of the elements where the nodes are located (yielding more inscribed area than the circle); (b) equating the radius of the circle to the radial distance locating the endpoints of the elements (giving less inscribed area than the circle); (c) adjusting the radial distance of the nodes so that the area of the defining circle is preserved. The idea is that as the number of elements increases, the three discretizations should converge to the same geometry, as should the results.

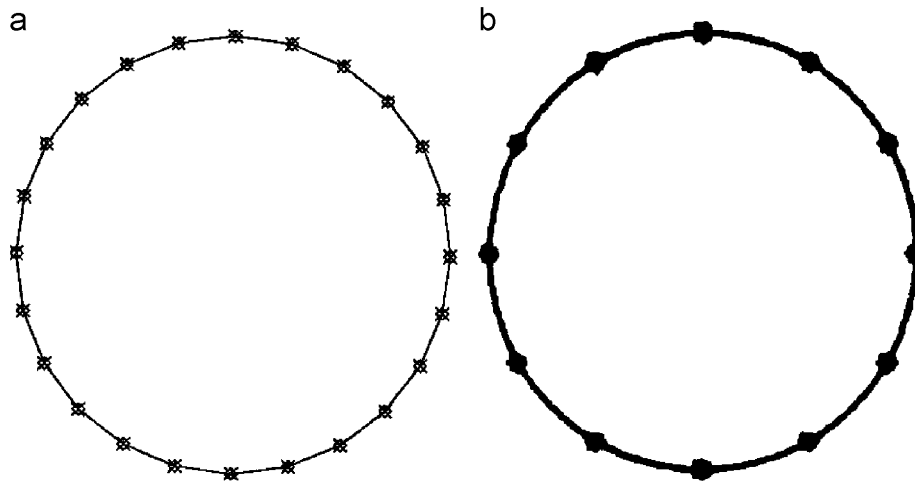


Fig. 1. Circular BEM discretization for (a) 24 constant or linear elements or (b) 12 Overhauser cubic elements [3].

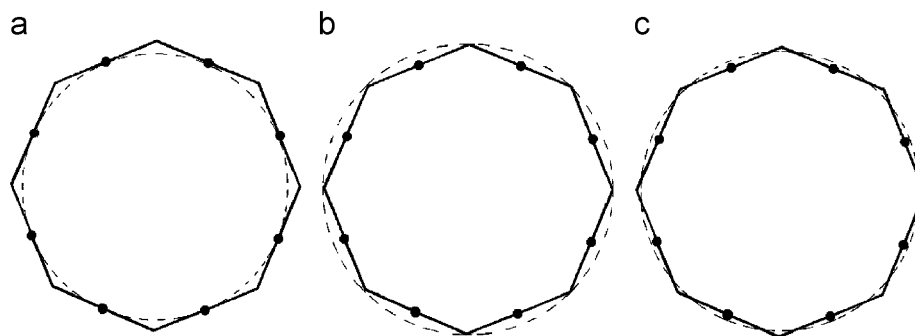


Fig. 2. Three ways of approximating a circle with eight constant elements of equal size. (a) the radial distance to the midside of an element is the same as the radius of the circle; (b) the radial distance to the endpoints of the elements is the same as the radius of the circle; (c) the interior area of the polygon is made to be the same as that for the circle.

The test case was a unit circle, $R = 1$, in Eqs. (11) and (12), zero values of u on the boundary (homogeneous Dirichlet conditions), and with the Poisson constant $B_0 = 1$. The formulation described in the previous section was used and results were first obtained using between 16 and 1000 constant elements. The results were very disappointing. They may be viewed in Table 1 in the rows indicated by a “ K value” of 1. (The explanation of the K value will be explained in a following section.) In each of the three geometrical criteria, there appears to be convergence to some value for the normal derivative but none are approaching the proper value of $q = 0.5$.

After coding errors were ruled out as being responsible for the poor performance, it was suspected that the quality of the element was at fault and higher order elements were tried. However, the results became progressively worse as the sophistication of the elements became better. The best results were expected to come from the Overhauser cubic spline element, which models the circular geometry most accurately due to its ability to maintain a smooth surface (C^1 inter-element continuity) [3]. However, it produced what could almost be interpreted as random numbers for

the fluxes. None of the explicit results for the higher-order elements are worth presenting here.

It was at this stage that an instability in the formulation was suspected and the results in the next section were derived.

4. The reason for the problem

For this particular problem, the final linear system of simultaneous equations for solution, represented by Eq. (10), follows from Eq. (1) to be simply

$$[G]\{q\} = -\{B\} \quad (13)$$

due to the values of u on the boundary being identically zero. Also, since every boundary node follows the same formulation as any of the others for equal elements, all the B_i are identical. With $b(x, y) = B_0 = \text{constant}$, we may compute the exact value for a boundary point B using Eq. (8) and the aid of Fig. 3.

Note that point B can represent any given boundary point with no loss of generality. Explicit calculation

Table 1
Unit circle results for the Poisson equation using equal length constant elements, homogeneous Dirichlet boundary conditions, and $b(x, y) = 1$

K value	Number of elements	Calculated derivative at boundary		
		Midside radial distance preserved	Endpoint radial distance preserved	Area of circle preserved
1	16	0.06207	0.59773	1.14470
1	24	0.04269	0.60107	1.09085
1	32	0.03253	0.60179	1.06644
1	64	0.01668	0.60168	1.03254
1	128	0.00844	0.60115	1.01709
1	192	0.00566	0.60095	1.01257
1	250	0.00435	0.60088	1.01079
1	500	0.00216	0.60096	1.00963
1	1000	0.00109	0.60150	1.01340
2	16	0.53054	0.52126	0.52741
2	24	0.52057	0.51639	0.51917
2	32	0.51549	0.51312	0.51470
2	64	0.50778	0.50719	0.50758
2	128	0.50380	0.50375	0.50385
2	192	0.50260	0.50253	0.50258
2	250	0.50200	0.50196	0.50199
2	500	0.50100	0.50099	0.50100
2	1000	0.50050	0.50050	0.50050
3	16	0.53157	0.52194	0.52833
3	24	0.52100	0.51672	0.51957
3	32	0.51573	0.51332	0.51492
3	64	0.50784	0.50724	0.50764
3	128	0.50391	0.50376	0.50386
3	192	0.50261	0.50254	0.50258
3	250	0.50200	0.50196	0.50199
3	500	0.50100	0.50099	0.50100
3	1000	0.50050	0.50050	0.50050
10	64	0.50789	0.50728	0.50769
10	250	0.50201	0.50197	0.50199

gives

$$\begin{aligned}
 B_i &= \int_{\Gamma} b \vec{\nabla} v_i^* \cdot \vec{n} d\Gamma = B_0 \int_{\Gamma} \frac{\partial v_i^*}{\partial r} \hat{e}_r \cdot \hat{e}_n d\Gamma \\
 &= B_0 \int_0^{2\pi} \frac{\partial}{\partial r} \left[\frac{r^2}{8\pi} (\ln r - 1) \right] \cos \frac{\theta}{2} R d\theta \\
 &= \frac{B_0 R}{8\pi} \int_0^{2\pi} r(2 \ln r - 1) \cos \frac{\theta}{2} d\theta \\
 &= \frac{B_0 R}{8\pi} \int_0^{2\pi} 2R \cos \frac{\theta}{2} \left[2 \ln \left(2R \cos \frac{\theta}{2} \right) - 1 \right] \cos \frac{\theta}{2} d\theta \\
 &= \frac{B_0 R^2}{2\pi} \int_0^{\pi} [2 \ln(2R \cos \psi) - 1] \cos^2 \psi d\psi
 \end{aligned}$$

or $B_i = \frac{B_0 R^2}{2} \ln R.$ (14)

We see that if $R = 1$, Eq. (14) gives rise to a homogeneous system for Eq. (13) which is normally a prelude to an eigenvalue problem. The standard boundary

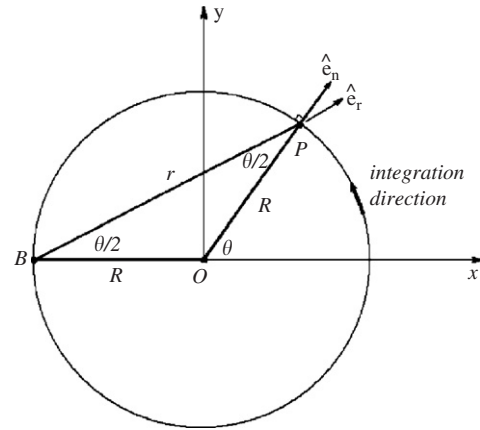


Fig. 3. Geometry for computing the Poisson term at a boundary point B.

element code, not being programmed for this contingency, will attempt to solve the system by inverting the $[G]$ matrix. Because of the inexactness of the discretization, the B_i will not be quite zero, and numerical instability, as the mesh is graded more finely, is most certain to ensue. This explains the apparent convergence to the different, but erroneous, $K = 1$ values in Table 1 as the radial criteria were changed. It also explains the diminishment in performance as the higher-order elements were implemented, since they will better approximate the exact zero values of B_i .

It should be noted that it is *not* the boundary integral formulation that is at fault, but rather the way typical coding is programmed that is the culprit. Boundary integral theory accurately predicts the correct result as can be illustrated with this same example:

Since all the equations represented by (13) are identical, and it is known that the q values are all the same, the entire system may be represented by the single exact (non-discretized) statement

$$\left(\int_{\Gamma} u_i^* d\Gamma \right) q = B_i, \tag{15}$$

where B_i is the exact value from Eq. (14). The boundary integral in Eq. (15) may be done explicitly by again enlisting the aid of Fig. 2

$$\int_{\Gamma} u_i^* d\Gamma = \int_{\Gamma} \frac{1}{2\pi} \ln r d\Gamma = \frac{1}{2\pi} \int_0^{2\pi} \ln \left(2R \cos \frac{\theta}{2} \right) R d\theta = R \ln R. \tag{16}$$

With this value, Eq. (15) becomes

$$(R \ln R)q = \frac{B_0 R^2}{2} \ln R$$

and the proper solution for any value of R is $q = B_0 R/2$ which agrees with the exact solution given by Eq. (12). Of course, a BEM program will not normally perform an eigenvalue analysis or take limiting values of R in order to effect a solution. Rather, it will attempt what is almost a zero by zero division in this last step.

5. A solution to the problem

Boundary element practitioners acquainted with the troublesome unit circle are usually aware that rescaling the geometry so as to avoid the problem with the logarithmic potential is a quick remedy. This is equivalent to a coordinate transformation [4]. This expedient may be formalized by recognizing that the usual fundamental solution utilized, Eq. (3), is incomplete. The proper fundamental solution is relative and allows for an additive constant C :

$$u_{K_i}^* = u_i^* + C = \frac{1}{2\pi} \ln |\vec{r} - \vec{r}_i| + C. \quad (17)$$

For neatness, we choose to rewrite the constant as $C = (1/2\pi)\ln K$ where K may be interpreted as a scaling factor. This renders Eq. (17) as

$$u_{K_i}^* = \frac{1}{2\pi} \ln(K|\vec{r} - \vec{r}_i|) \quad (18)$$

and we see that K magnifies the radial distance. With Eq. (18) used in place of Eq. (3) and also to rederive Eq. (9), the equivalent calculations leading up to Eqs. (14) and (16) give

$$B_i = (B_0 R^2/2) \ln KR \quad \text{and} \quad \int_{\Gamma} u_{K_i}^* d\Gamma = R \ln KR \quad (19)$$

and it is readily verified that choosing K to be any positive value other than unity will eliminate the problem that occurs when $K=1$. This result is illustrated in Table 1 for several constant mesh refinements when $K=2$ and 3 and for a pair of cases when $K=10$. The calculated values of the boundary derivatives indicate deviations which gradually decrease monotonically as the discretization is refined. This performance is consistent with what can normally be expected for the elementary constant element. Pragmatic convergence of the results seems to have occurred in the neighborhood of 250 elements when $K \neq 1$.

A refined test for many values of K ranging between 0.01 and 1.5 was performed to study the sensitivity of the instability. These results are presented in Table 2. The poor behavior seems to be very localized at values of K in the range of 1 ± 0.0005 . This is an encouraging result since it indicates a suspected problem with instability can be resolved quite easily by adjusting the value of K only slightly.

6. Further considerations

Several other cautions with this type of instability should be observed. For one, we can see that using Eq. (18) sidesteps the unit circle trap but it has the potential of creating one elsewhere. In Eqs. (19) for instance, it can be seen that if K is chosen accidentally so that $K=1/R$, the problem with instability can occur for any arbitrary value of the radius.

Table 2
Detailed study of the sensitivity to the K value

Number of elements	K Value	Calculated derivative at boundary for the case when the circular area is preserved	Percentage difference between calculated and exact (%)
128	0.01	0.503892	0.78
128	0.1	0.503897	0.78
128	0.2	0.503901	0.78
128	0.3	0.503896	0.78
128	0.4	0.503914	0.78
128	0.5	0.503923	0.78
128	0.6	0.503936	0.79
128	0.7	0.503957	0.79
128	0.8	0.503999	0.80
128	0.9	0.504127	0.83
128	0.91	0.504155	0.83
128	0.92	0.504190	0.84
128	0.93	0.504235	0.85
128	0.94	0.504295	0.86
128	0.95	0.504379	0.88
128	0.96	0.504506	0.90
128	0.97	0.504716	0.94
128	0.98	0.505136	1.03
128	0.99	0.506392	1.28
128	0.995	0.508886	1.78
128	0.9995	0.549950	9.99
128	0.99995	0.758719	51.74
128	0.999995	0.969850	93.97
128	0.9999995	1.011942	102.39
128	1	1.017093	103.42
128	1.0000005	1.022349	104.47
128	1.000005	1.074995	115.00
128	1.000049	80.263400	15,952.68
128	1.0000491	116.962074	23,292.41
128	1.0000492	216.213748	43,142.75
128	1.0000493	1460.483820	29,1996.76
128	1.00004931	3450.571850	690,014.37
128	1.00004932	-9501.389290	1,900,377.86
128	1.00004935	-774.379471	-154,975.89
128	1.0000494	-305.683446	-61,236.69
128	1.0000495	-138.059966	-27,711.99
128	1.0000496	-89.039233	-17,907.85
128	1.0000497	-65.639287	-13,227.86
128	1.0000498	-51.935511	-10,487.10
128	1.0000499	-42.9355711	-8687.11
128	1.00005	-36.572344	-7414.47
128	1.000051	-14.538103	-3007.62
128	1.0001	0.004480	-99.10
128	1.00025	0.377751	-24.45
128	1.0005	0.447713	-10.46
128	1.003	0.495296	-0.94
128	1.005	0.498761	-0.25
128	1.01	0.501330	0.27
128	1.05	0.503367	0.67
128	1.5	0.503824	0.76

These are unit circle results for the Poisson equation using 128 equal length constant elements, homogeneous Dirichlet boundary conditions, and $b(x, y) = 1$. The exact value is $q = 0.5$.

Also, the possibility for a similar problem occurring on an *arbitrarily shaped* bounded domain Ω must be considered. Linear algebra theory tells us it is always possible

to construct a function $b(x, y)$ which will be orthogonal to a given function in an inner product space (for boundary element analysis, this will most often be a Euclidean vector space). Thus, by sheer happenstance, there always exists the possibility that

$$B_i = \int_{\Omega} u_i^* b(x, y) d\Omega \equiv 0$$

for any bounded domain Ω , and the “unit circle trap” can become a more general geometrical trap when homogeneous boundary conditions are present. At this writing, there does not appear to be any complete set of conditions that will allow the analyst to predict a priori when the problem will occur. (This issue will be addressed in the next section.) For this reason, the empirical device of using the fundamental solution (18) with several different values of the K parameter seems to be the best approach for handling a suspected instability.

The close relationship of the Poisson equation to Laplace’s equation can make the problem occur in a more subtle manner. While much attention has been given transformation of Poisson’s equation to Laplace’s equation, it is also true that the reverse can be done as well. Starting with the Dirichlet problem

$$\begin{aligned} \nabla^2 w(x, y) &= 0 \quad \text{in } \Omega, \\ w &= \bar{w} \quad \text{on } \Gamma, \end{aligned} \tag{20}$$

it is most likely possible, in principle at least, to find a function $b(x, y)$ such that $\nabla^2 \bar{w} = b$. Letting $u = w - \bar{w}$, This boundary value problem defined by Eq. (20) may be recast as

$$\begin{aligned} \nabla^2 u &= b(x, y) \quad \text{in } \Omega, \\ u &= 0 \quad \text{on } \Gamma, \end{aligned}$$

which is precisely the Poisson equation with homogeneous boundary conditions.

This result means that we can look at the problem from the viewpoint of a Laplacian solution. The separation of variables solution for Laplace’s equation on a circle of radius R is

$$u(R, \theta) = \sum_{n=0}^{\infty} [a_n \cos n\theta + b_n \sin n\theta] \left(\frac{r}{R}\right)^n. \tag{21}$$

The famous *Poisson integral solution* follows from either manipulation of this formula or from the Cauchy integral theorem [5]:

$$u(r, \theta) = \frac{1}{2\pi} \int_0^{2\pi} \left[\frac{R^2 - r^2}{R^2 - 2rR \cos(\theta - \alpha) + r^2} \right] u(R, \alpha) d\alpha. \tag{22}$$

Eq. (22) is the solution to the interior Dirichlet problem on a circle; the term in square brackets is called the *Poisson kernel*. As to its relevance in this paper, we can interpret the Poisson integral solution as finding the potential u at (r, θ) as a *weighted average* of the boundary potentials $u(R, \theta)$ weighted by the Poisson kernel.

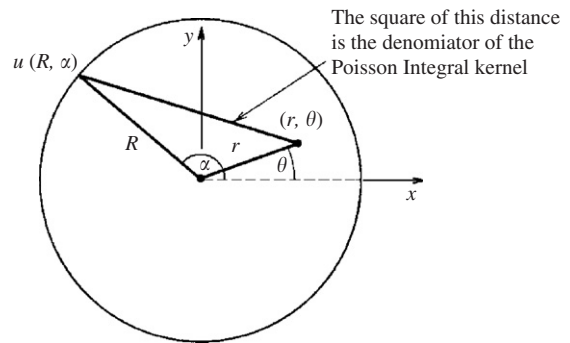


Fig. 4. $u(r, \theta)$ interpreted as a weighted sum of boundary potentials due to the Poisson kernel.

The interpretation about the underlying physical system is that the potential at a point is the weighted average of neighboring potentials. The Poisson kernel dictates the weight assigned to each point. For boundary values $u(R, \alpha)$ close to (r, θ) , the Poisson kernel gets large, since the denominator of the Poisson kernel is the square of the distance from (r, θ) to (R, α) as shown in Fig. 4. Due to this fact, the integral puts more weight on those values of $u(R, \alpha)$ that are closest to (r, θ) . Unfortunately, if (r, θ) is extremely close to the boundary $r = R$, then the Poisson kernel gets very large for those values of α that are closest to (r, θ) . For this reason, when point (r, θ) is close to the boundary, it is known that the series solution, Eq. (21), works better for evaluating the numerical value of the solution. Taking (r, θ) on the boundary is precisely what happens in the boundary element formulation; the similarity of Figs. (3) and (4) should be apparent. It is thus demonstrated that the problems with the two integral statements are equivalent.

7. Other discussions of the unit circle trap

It was mentioned earlier that the background sources alluding to this problem were transmitted mostly by private communications. However, literary sources that used terminology different than that of the “trap,” coined in this work, were pointed out after the publication of the authors’ conference paper [1]. The text by Jaswon and Symm [6] discusses work previously published by Jaswon [7] and further credits Petrovsky [8] with discovering this troublesome feature of the unit circle as early as 1954. Jaswon and Symm [6] describe the existence of curves called Γ -contours for which expressions of the form (15) have no solution. Particularly a circle of unit radius yields as feasible solutions any finite values of the normal derivatives.

They also point out that the notion of the problem with the unit circle may be generalized to any Cartesian contour defined by $f(x, y) = 0$. They prove that given such a contour, the family of similar contours defined by $f(x/m, y/m) = 0$, where $m > 0$ is a continuously varying parameter, each admits a unique solution for the normal derivatives q except for one, that being the Γ -contour which will create the

problem. Thus, no closed contour in the Cartesian plane is immune from yielding a possible instability when the Poisson equation with zero potentials is analyzed.

More recently, Chen et al. [9,10] addressed the similar problem showing up in the Laplace equation and annular regions and other special geometries. The term used by them for a generic unit circle trap is “degenerate scale.” The exhaustive analytical and numerical experiments overlap somewhat with the more concise presentation given here in Section 6.

8. Discussion and conclusions

The unit circle with homogeneous boundary conditions in the boundary element method has been shown to institute a numerical stability problem in the Poisson equation. While admittedly the unit circle trap is an isolated instance, it is troublesome for at least three reasons. First, the trap may not manifest itself as an obvious instability. For instance, if only one of the radial criteria had been instituted in construction of the $K = 1$ results in Table 1, and the correct result had not been known a priori, then it would have been very easy to have concluded that the results were converging with increased mesh refinement. Such a premature conclusion can obviously be dangerous. Secondly, if the problem can occur with the Poisson equation on the unit circle, it can possibly occur with other geometries, boundary conditions, and governing equations in more subtle ways not as easily detected. The underlying problem lies in the nature of the logarithmic potential, which shows up not only in two-dimensional potential theory but also in elastostatics. The elasticity problem of this nature has been addressed by Chen et al. [11]. Other fundamental potentials may create similar problems. Thirdly, and most simply, circular geometries are quite common occurrences in practice.

Proposed here is a formal remedy that involves rescaling using the additive constant available in the full form of the fundamental solution for the Laplacian operator. Other basic solutions to the underlying problem exist, the most efficacious of which might be exploiting the symmetry of the geometry. For instance, modeling a one-quarter sector of the unit circle domain and using the no-flux boundary conditions on the straight sides gives very good results with

the unscaled version of the fundamental solution. This is due to the mixed boundary value nature of the synthesis.

This work shows that it may be futile to try predict *a priori* when a problem with a vanishing Poisson term may cause a numerical instability. Though the unit circle seems to be the most vulnerable to this type of problem (probably due to its frequent occurrence), the instability can occur on any arbitrary closed domain. The full form of the fundamental solution given by either Eq. (17) or Eq. (18) should be respected and used appropriately. The empirical means of dealing with the problem is to evaluate the solution for several values of the scaling factor K .

References

- [1] Gipson GS, Yeigh BW. The unit circle trap in boundary elements. In: Boundary elements XXVII incorporating electrical engineering and electromagnetics. Southampton: WIT Press; 2005. p. 501–9.
- [2] Gipson GS. Boundary element fundamentals—basic concepts and developments in the Poisson equation. Southampton: Computational Mechanics Publications; 1987. p. 108–149.
- [3] Ortiz JC, Walters HG, Gipson GS, Brewer III JA. Development of overhauser splines as boundary elements. In: Brebbia CA & Wendland WL., editors. Boundary elements IX: mathematical and computational aspects, vol. 1. Proceeding of the ninth international conferences on boundary element methods. Berlin: Springer-Verlag and Southampton: Computational Mechanics Institute; 1987. p. 401–7.
- [4] Brebbia CA. Personal communication, 26 May 2004, Director, Wessex Institute, Ashurst Lodge, Ashurst, Southampton, UK.
- [5] Wylde HW. Mathematical methods for physics. Reading, MA: Benjamin/Cummings Publishing Company, Inc.; 1976. p. 446–7.
- [6] Jaswon MA, Symm GT. Integral equation theory in potential theory and elastostatics. London: Academic Press; 1977. p. 52–4.
- [7] Jaswon MA. Integral equation methods in potential theory. I. Proc Roy Soc (A) 1963;273:23–32.
- [8] Petrovsky IG. Lectures on partial differential equations. New York: Interscience; 1954.
- [9] Chen JT, Lin JH, Kuo SR, Chiu YP. Analytical study and numerical experiments for degenerate scale problems in boundary element method using degenerate kernels and circulants. Eng Anal Bound Elem 2001;25:819–28.
- [10] Chen JT, Lee CF, Chen IL, Lin JH. An alternative method for degenerate scale problems in boundary element methods for the two-dimensional Laplace equation. Eng Anal Bound Elem 2002;26: 559–69.
- [11] Chen JT, Kuo SR, Lin JH. Analytical study and numerical experiments for elasticity plane problem with degenerate scale problems in boundary element method. Int J Numer Meth Eng 2002; 54:1669–81.